The Fc Segment of IgE Influences the Kinetics of Dissociation of a Symmetrical Bivalent Ligand from Cyclic Dimeric Complexes†

Kala Subramanian,‡ David Holowka,*,‡ Barbara Baird,*,‡ and Byron Goldstein*,§

Department of Chemistry, Baker Laboratory, Cornell University, Ithaca, New York 14853, and Theoretical Biology and Biophysics Group, Theoretical Division, T-10, MS K710, Los Alamos National Laboratory, Los Alamos, New Mexico 87545

Received October 2, 1995; Revised Manuscript Received February 5, 1996⊗

ABSTRACT: As part of a systematic effort to determine the features of immunoglobulin E−receptor (IgE−FcεRI) aggregation that are critical for cellular activation, we used fluorescence to examine the dissociation of a soluble bivalent ligand, *N,N′*-bis[[ε-[(2,4-dinitrophenyl)amino]caproyl]-L-tyrosyl]-L-cystine ((DCT)$_2$-cys), from soluble bivalent IgE and its bivalent F(ab′)$_2$ and monovalent Fab′ fragments. Cross-linking of Fab′ fragments by (DCT)$_2$-cys is limited to linear dimers, and we find that (DCT)$_2$-cys dissociation from Fab′ occurs with a single kinetic coefficient [$(4.2 \pm 0.6) \times 10^{-3}$ s^{-1}] that corresponds to the lower of the two kinetic coefficients observed with the bivalent IgE [$(4.7 \pm 0.7) \times 10^{-2}$ s^{-1} and $(4.4 \pm 0.3) \times 10^{-3}$ s^{-1}]. Similarly, the lower value is obtained for dissociation of (DCT)$_2$-cys that is monovalently bound to IgE after incubation with a large excess of the ligand. (DCT)$_2$-cys can bind to bivalent F(ab′)$_2$ fragments and form a variety of linear and cyclic aggregates, similarly to IgE, but, unlike IgE, we find that dissociation occurs with a single kinetic coefficient similar to that observed for Fab′. We find that IgE and its (Fab′)$_2$ fragments form highly stable cyclic dimer rings with two (DCT)$_2$-cys. We demonstrate that the kinetic coefficients are independent of enhanced fluorescence quenching observed for bound sites in cyclic dimers. Together, the results show that the rate constant for breaking a linear cross-link formed by (DCT)$_2$-cys is the same as that for dissociation of the monovalently bound (DCT)$_2$-cys. Further, they show that opening of a bond in a dimer ring for the F(ab′)$_2$ fragment occurs with approximately the same dissociation rate constant as opening a bond in a linear cross-link. This rate constant is about three times smaller than that observed with IgE, suggesting that steric strain is caused by apposed Fc segments in cyclic IgE dimers. Such structural interference may affect the functional consequences of IgE−FcεRI aggregation on the cell surface.

Antigen-mediated aggregation of IgE bound to its high-affinity receptor (FcεRI) on the surface of mast cells and basophils initiates signal transduction leading to cellular activation and release of chemical mediators in the allergic response. Although cross-linking of IgE−FcεRI is required for signaling, not all cross-linking is equally effective. Little is known about the critical structural and dynamic features that make an IgE−FcεRI aggregate a robust signaling unit. We have developed an experimental system with well-defined ligands to address this problem that includes soluble IgE as well as IgE bound to FcεRI on cell membranes. Because IgE in solution has a bent conformation (Zheng et al., 1992; Beavil et al., 1995) that is retained when IgE binds to FcεRI on cells (Zheng et al., 1992), information about the binding and cross-linking of IgE by ligands in solution is relevant for understanding the more complicated cell surface events. Our binding studies have focused on a symmetrical bivalent ligand because it represents the simplest ligand that causes IgE aggregation.

The experiments described here extend previous studies with the murine mAb IgE that is specific for 2,4-dinitrophenyl (DNP)-ligands (Liu et al., 1980). The symmetrical bivalent ligand employed is *N,N′*-bis[[ε-[(2,4-DNP)amino]-caproyl]-L-tyrosyl]-L-cystine ((DCT)$_2$-cys),[1] which effectively cross-links IgE in solution and IgE bound to FcεRI on RBL mast cells (Erickson et al., 1986, 1991; Kane et al., 1986; Posner et al., 1991). We showed previously that (DCT)$_2$-cys dissociates from IgE in solution with a faster (4.8×10^{-2} s^{-1}) and a slower (5.6×10^{-3} s^{-1}) kinetic coefficient[2,3] (Posner et al., 1991), and similar numbers were obtained with IgE bound to cells (Erickson et al., 1991). Those two binding studies suggested that (DCT)$_2$-cys forms highly stable cyclic dimers (containing two (DCT)$_2$-cys and two IgE) that could prevent the generation of larger cross-linked aggregates. In a subsequent study (Posner et al., 1995), this propensity to form cyclic dimers on the cell surface was determined to be the cause of the severely limited functional response to this ligand.

In order to identify the molecular events occurring with (DCT)$_2$-cys and IgE that correspond to the measured faster

† Work supported by National Institutes of Health Research Grants GM35556 and AI22449, by National Science Foundation Grant GER-9023463, and by the United States Department of Energy.

* Authors to whom correspondence should be addressed.
‡ Cornell University.
§ Los Alamos National Laboratory.

⊗ Abstract published in *Advance ACS Abstracts,* April 15, 1996.

[1] Abbreviations: IgE, immunoglobulin E; DNP, 2,4-dinitrophenyl; DCT, [ε-[(2,4-DNP)amino]caproyl]-L-tyrosine; (DCT)$_2$-cys, *N,N′*-bis-[DCT]-L-cystine.

[2] The term *kinetic coefficient* refers to the apparent rate constant, which includes statistical factors, that appears in the exponent of exponential decay curves used to the fit the data. For example, k_{-1} and $4j_{-2}$ are the kinetic coefficients appearing within the double-exponential expression of eq 6.

[3] $(4.8 \pm 3.2) \times 10^{-2}$ s^{-1} and $(5.6 \pm 1.9) \times 10^{-3}$ s^{-1} are the arithmetic average values for the two kinetic coefficients[2] from eight dissociations experiments with IgE and (DCT)$_2$-cys listed in Table 1 of Posner et al. (1991).

S0006-2960(95)02352-X CCC: $12.00

and slower dissociation constants, we have now compared the binding of $(DCT)_2$-cys to soluble IgE with its binding to $F(ab')_2$ and Fab fragments. Our results identify the faster dissociation event as the opening of the cyclic dimers, and they further reveal that the Fc segment can influence the dissociation rate of the cross-linked cyclic dimer state. The implications of these results for the structure−function relationships of cross-linked IgE−FcϵRI on the cell surface are considered.

MATERIALS AND METHODS

Reagents. Fluorescein 5′-isothiocyanate (FITC) was obtained from Molecular Probes, Inc. (Eugene, OR). The monovalent ligand, [ϵ-[(2,4-dinitrophenyl)amino]caproyl]-L-tyrosine (DCT), was obtained from Biosearch, Inc. (San Rafael, CA), and the bivalent ligand, $(DCT)_2$-cys (M_r ~1000), was synthesized and characterized in this laboratory as described previously (Kane et al., 1986). The $(DCT)_2$-cys was further purified from the TLC isolate (Kane et al., 1986) with a reverse phase C_{18} column and a gradient of 5% methanol/95% 1 mM triethylamine phosphate (pH 6.7) to 100% methanol in a Waters HPLC system. DNP peaks were detected by absorbance at 340 nm, and $(DCT)_2$-cys was identified as the major HPLC peak eluting at ~63% methanol.

IgE and Derivatives. The anti-DNP IgE was affinity-purified from hybridoma H1 26.82 (Liu et al., 1980) as previously described (Holowka & Baird, 1983). Final steps in the purification included ion exchange chromatography to remove bound DNP-L-glycine and gel filtration chromatography to isolate the monomeric form of IgE from any aggregates (Posner et al., 1991). The modification of IgE with FITC has been described (Erickson et al., 1986). The stoichiometry of labeling was typically 8 FITC fluorophores per IgE.

$F(ab')_2$ and Fab′ fragments of FITC-IgE were prepared by a method modified from Perez-Montfort and Metzger (1982). For the $F(ab')_2$, FITC-IgE, dialyzed against Tris buffer (40 mM Tris, 2 mM $CaCl_2$, 50 mM NaCl, pH 8.1), was digested for 3 h at room temperature with DPPC-treated trypsin (Sigma Chemical Co.), dissolved in 1 mM HCl, that was added at a final concentration of 2% of the IgE (w/w). The reaction was stopped by adding 10-fold excess (w/w) of soybean trypsin inhibitor (Sigma) over trypsin. Fab′ was produced by reducing a portion of the unpurified $F(ab')_2$ with 5 mM dithiothreitol in Tris buffer at room temperature for 1 h, followed by alkylation with 12 mM *N*-ethylmaleimide.

$F(ab')_2$ and the Fab′ fragments were purified with a Superose 12 HPLC gel filtration column (Pharmacia Fine Chemicals); elution was with a phosphate/sulfate buffer (20 mM sodium phosphate, 0.1 M sodium sulfate, 0.02% NaN_3, pH 7.4) at a flow rate of 0.5 mL/min (Figure 1). Comparison of retention times with those of known protein standards (BioRad, Melville, NY) indicated that the fragments eluted as expected for their respective molecular masses. Peak fractions of the $F(ab')_2$ and Fab′ preparations were used in the binding experiments. The purity of the fragments was confirmed by SDS−PAGE with 10% acrylamide, under reducing and non-reducing conditions, and staining with Coomassie Brilliant Blue R-250 (Bio-Rad) (data not shown). The stoichiometries of labeling for the IgE fragments were determined by absorption spectroscopy (Erickson et al., 1986) to be 3.0 FITC fluorophores per $F(ab')_2$ and 1.8 FITC fluorophores per Fab′. In all experiments described here the concentrations of the IgE and Fab′ and $F(ab')_2$ fragments were determined according to their binding sites as titrated with DCT (Erickson et al., 1986).

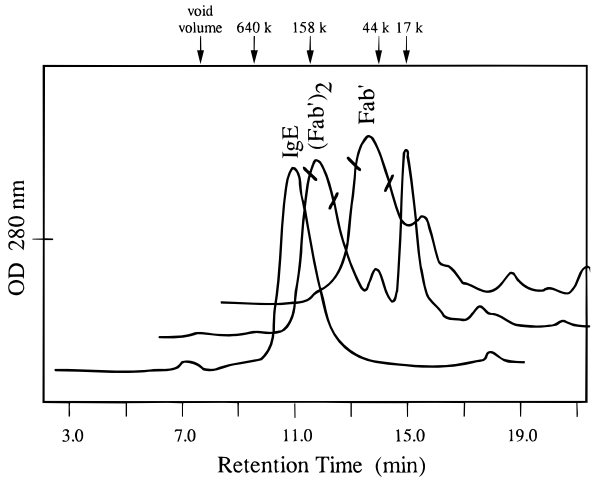

FIGURE 1: Superose 12 gel filtration chromatography of FITC-IgE, FITC-IgE $F(ab')_2$, and FITC-IgE Fab′ fragments. The peak fractions of $F(ab')_2$ and Fab′ indicated by the hatched marks were pooled for use in the dissociation experiments. The retention times and the molecular masses for standard proteins (thyroglobulin, γ-globulin, ovalbumin, and myoglobin) are indicated on the upper *x*-axis.

Gel filtration was used to analyze the size and type of cross-linked aggregates present after chromatographic separation of $F(ab')_2$ (0.4 μM; 0.8 μM sites) or intact IgE (0.5 μM; 1.0 μM sites) that had been pre-incubated for 30 min at room temperature with near-stoichiometric amounts of $(DCT)_2$-cys (0.35 μM) in the phosphate/sulfate buffer (0.6 mL total sample volume). For control samples, IgE (0.24 μM) and $F(ab')_2$ (0.12 μM) were chromatographed separately. All samples were analyzed with a 10 × 300 mm Superose 6 HPLC column (Pharmacia Fine Chemicals) in the phosphate/sulfate buffer at room temperature at a flow rate of 0.6 mL/min.

Spectrofluorimetric Measurements. As described previously (Erickson et al., 1986) these were made with an SLM 8000 fluorescence spectrophotometer operated in ratio mode. FITC-IgE, FITC-IgE $F(ab')_2$, or FITC-IgE Fab′ in 2 mL of buffered salt solution (BSS: 135 mM NaCl, 5 mM KCl, 1 mM $MgCl_2$, 1.8 mM $CaCl_2$, 5.6 mM glucose, 0.1% gelatin, 20 mM Hepes, pH 7.4) was maintained at 15 °C and stirred continuously. FITC was excited at 490 nm, and emission was monitored at 526 nm. Binding of the $(DCT)_2$-cys to the FITC-IgE (or fragments) is monitored by fluorescence quenching of FITC by bound DNP ligands (Erickson et al., 1986). The dissociation kinetics are observed by adding a large excess of DCT to equilibrated mixtures of IgE and $(DCT)_2$-cys and monitoring the resultant fluorescence recovery. DCT quenches FITC-IgE less than $(DCT)_2$-cys, and when the concentration of DCT is sufficiently high it fills all the remaining binding sites on the IgE and prevents the rebinding of $(DCT)_2$-cys as it dissociates (Posner et al., 1991). The fluorescence binding data were collected continuously with an AST 286 computer for subsequent analysis.

Data Analysis. The equilibrium theory for bivalent ligands binding to bivalent IgE has been described in detail previously (Dembo & Goldstein, 1978). Among other results, the theory predicts the total bivalent ligand concentration (C_{Tmax}) corresponding to maximal cross-linking at any

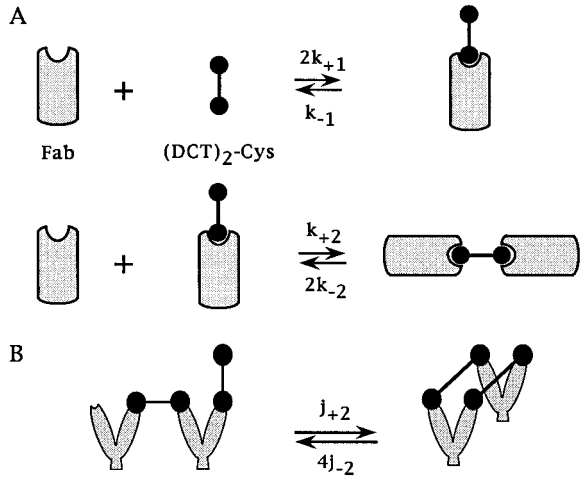

FIGURE 2: Mechanism for sequential binding of the bivalent ligand $(DCT)_2$-cys to IgE anti-DNP sites (represented at the ends of Fab segments). (A) Monovalent binding of $(DCT)_2$-cys is described by rate constants k_{+1} and k_{-1}. Crosslinking of Fab segments within IgE or F(ab′)$_2$ to form linear chains of any number of units is described by rate constants k_{+2} and k_{-2}. Fab fragments can be cross-linked only into dimers. (B) Further cross-linking of a linear dimer of F(ab′)$_2$ fragments or IgE (Fc segments not shown) to form a ring structure requires additional rate constants j_{+2} and j_{-2}.

concentration of IgE at equilibrium:

$$C_{\mathrm{Tmax}} = 1/(2K_1) + [\mathrm{IgE}]_{\mathrm{Total}} \quad (1)$$

For binding to monovalent Fab′ fragments eq 1 becomes

$$C_{\mathrm{Tmax}} = 1/(2K_1) + [\mathrm{Fab'}]_{\mathrm{Total}}/2 \quad (2)$$

where K_1 is the intrinsic equilibrium constant for monovalent binding of ligand. We previously established for $(DCT)_2$-cys, $K_1 = 2 \times 10^9$ M^{-1} such that $1/(2K_1) = 0.25$ nM (Erickson et al., 1986; Posner et al., 1995). In general, eq 1 applies to the formation of all types of aggregates, including linear and cyclic aggregates of all lengths. The theory allows calculation of the concentrations of these different types of aggregates at equilibrium if the appropriate equilibrium constants are known (Dembo & Goldstein, 1978; Goldstein, 1988).

If cyclic aggregates are not formed, the binding of the bivalent ligand to the two equivalent Fab binding sites of IgE in solution or on cell surfaces can be modeled as a two-step process (Figure 2A) (Posner et al., 1991; Erickson et al., 1991). The equivalent site approximation (Perelson & DeLisi, 1980) allows IgE cross-linked into linear chains of all lengths to be described by two sets of rate constants, k_{+1}, k_{-1} and k_{+2}, k_{-2}. In the presence of a large excess of monovalent ligand DCT, which fills up all free sites, the forward reactions in Figure 2A cannot occur, and the resulting dissociation is described by the two reverse rate constants, k_{-1} and k_{-2}. Under these conditions we obtain the following double-exponential expression for f_b, the fraction of initially bound sites that remain bound at time t (Posner et al., 1991):

$$f_b = A\exp(-k_{-1}t) + (1 - A)\exp(-2k_{-2}t) \quad (3)$$

$$A = 1 - a(k_{-1} - k_{-2})/(2k_{-1} - k_{-2}) \quad (4)$$

where A is the normalized pre-exponential weighting factor (i.e., the amplitude) and a is the fraction of sites occupied by doubly bound ligands at time $t = 0$. If the fluorescence quenching is the same for all bound sites, then the observed changes in the relative fluorescence (F) is given by

$$F = F_{\max} - (F_{\max} - F_{\min})[A\exp(-k_{-1}t) + (1 - A)\exp(-2k_{-2}t)] + st \quad (5)$$

where $F_{\max}$ is the value of the relative fluorescence after the dissociation has gone to completion (i.e., when all sites are filled by DCT), $F_{\min}$ is the relative fluorescence immediately after the addition of the DCT (i.e., when all free sites become filled with DCT but before dissociation of any bivalent ligand occurs), and s is a factor that accounts for any instrumental drift in the fluorescence over time. If the two ends of the bivalent ligand dissociate independently such that $k_{-1} = k_{-2}$, then eq 5 simplifies to a single-exponential expression:

$$F = F_{\max} - (F_{\max} - F_{\min})[\exp(-k_{-1}t)] + st \quad (6)$$

The scheme in combined Figure 2A,B includes the formation of dimers in rings containing two IgE and two bivalent ligands. This type of cyclic dimer aggregate requires an additional dissociation rate constant, j_{-2}, corresponding to the dissociation of a bond to open the ring. The complete equation for dissociation would then include three independent rate constants. However, in the case $k_{-1} = k_{-2}$, the equation for f_b corresponding to this dissociation contains two independent rate constants in the form of a double-exponential expression similar to eq 3:

$$f_b = A\exp(-k_{-1}t) + (1 - A)\exp(-4j_{-2}t) \quad (7)$$

where now

$$A = 1 - a(k_{-1} - 3j_{-2})(k_{-1} - j_{-2})/[(k_{-1} - 2j_{-2})(k_{-1} - 4j_{-2})] \quad (8)$$

and a is now the fraction of doubly bound ligands in cyclic dimers at $t = 0$. If the quenching is the same for all bound sites, then

$$F = F_{\max} - (F_{\max} - F_{\min})[A\exp(-k_{-1}t) + (1 - A)\exp(-4j_{-2}t)] + st \quad (9)$$

Note that eqs 3 and 5 have forms identical to eqs 7 and 9, respectively, except that $-2k_{-2}$ is replaced by $-4j_{-2}$ as the kinetic coefficient in the second exponential term, with the integer representing the appropriate statistical factor. If $k_{-1} = k_{-2} = j_{-2}$, then eq 9 simplifies to the single-exponential expression of eq 6.

If a bound site in a cyclic complex quenches differently from other bound sites, eq 9 is still correct, but A no longer is given by eq 8. In addition to depending on the rate constants and the fraction of doubly bound ligands in cyclic dimers at $t = 0$, A will now depend on the differences in quenching between the different types of bound states. In the Appendix we discuss this in detail and present evidence indicating that in our system a site bound in a cyclic complex quenches more strongly than other bound sites. It is important to note that, as demonstrated in the Appendix, the values of the kinetic coefficients determined with these equations and nonlinear least-squares fitting of the data are

unaffected by any differences in quenching for different bound states.

The binding data were fit with either eq 6 or eq 9. The values for the parameters were obtained using a subroutine, DNLSI, from the Common Los Alamos Software Library which is based on a finite difference, Levenberg−Marquardt algorithm for solving nonlinear least-squares problems.

RESULTS

Dissociation Kinetics. In order to evaluate the binding scheme shown in Figure 2 and to identify the dissociation events corresponding to the observed kinetic coefficients,[2] we compared the dissociation of $(DCT)_2$-cys from intact IgE and its $F(ab')_2$ and Fab′ fragments. IgE and $F(ab')_2$ are bivalent and can, in principle, form both linear and cyclic aggregates of various sizes when combined with bivalent ligands. Fab′ can cross-link only into linear dimers with $(DCT)_2$-cys. Dissociation of linear chains of all lengths can be described by two dissociation constants, k_{-1} and k_{-2} (Figure 2A); inclusion of the cyclic dimer requires a third constant, j_{-2} (Figure 2B). In our experiments $(DCT)_2$-cys was first incubated with FITC-labeled anti-DNP IgE until binding was complete or near-complete. Then excess DCT was added to fill all free IgE binding sites and prevent further forward binding of $(DCT)_2$-cys, thus allowing its net dissociation to be monitored. To maximize cross-linking we used near stoichiometric amounts of $(DCT)_2$-cys and IgE in the initial incubation mixture (eq 1).

The dissociation of $(DCT)_2$-cys from FITC-IgE after stoichiometric incubation is shown by the representative data in Figure 3A. As expected from previous studies (Posner et al., 1991) these data are well-fitted by a double-exponential equation (eq 6 or 9), with a faster (3.7×10^{-2} s^{-1}) and a slower (4.0×10^{-3} s^{-1}) kinetic coefficient.[2] As described in the Appendix, these kinetic coefficients are independent of differential quenching occurring with bound sites in cyclic dimers compared to other types of bound sites. Six similar experiments with IgE and $(DCT)_2$-cys yielded average values for these kinetic coefficients of $(4.7 \pm 0.7) \times 10^{-2}$ s^{-1} and $(4.4 \pm 0.3) \times 10^{-3}$ s^{-1} (data not shown). A single-exponential equation (eq 4) provides a poor best fit of each of these data sets that deviates most markedly from the data at the fast, early phase of the recovery curve as revealed by the calculated residuals (data not shown). The results obtained with $(DCT)_2$-cys and IgE can be interpreted with the binding steps depicted in Figure 2A, assuming $k_{-1} \neq k_{-2}$ (eq 5). Alternatively, they are consistent with the combination of the binding steps included in Figure 2A,B, assuming $k_{-1} = k_{-2} \neq j_{-2}$ (eq 9). Our previous studies with IgE bound to FcϵRI on RBL cells provided strong evidence for highly stable cyclic dimers (Posner et al., 1995), consistent with the suggestion that eq 9 is also the most appropriate for IgE in solution (Posner et al., 1991). Definitive assignment of the two rate constants to the two experimentally determined values for IgE in solution requires further information. For this purpose we investigated $(DCT)_2$-cys dissociation from IgE-Fab′, for which cross-linking is limited to linear dimers.

In contrast to the results obtained with intact IgE, dissociation of $(DCT)_2$-cys from IgE-Fab′ (Figure 3B) occurs as a single-exponential process and can be described by eq 6. When the data are fitted with two exponentials there is no significant decrease in the sum of squares. The single

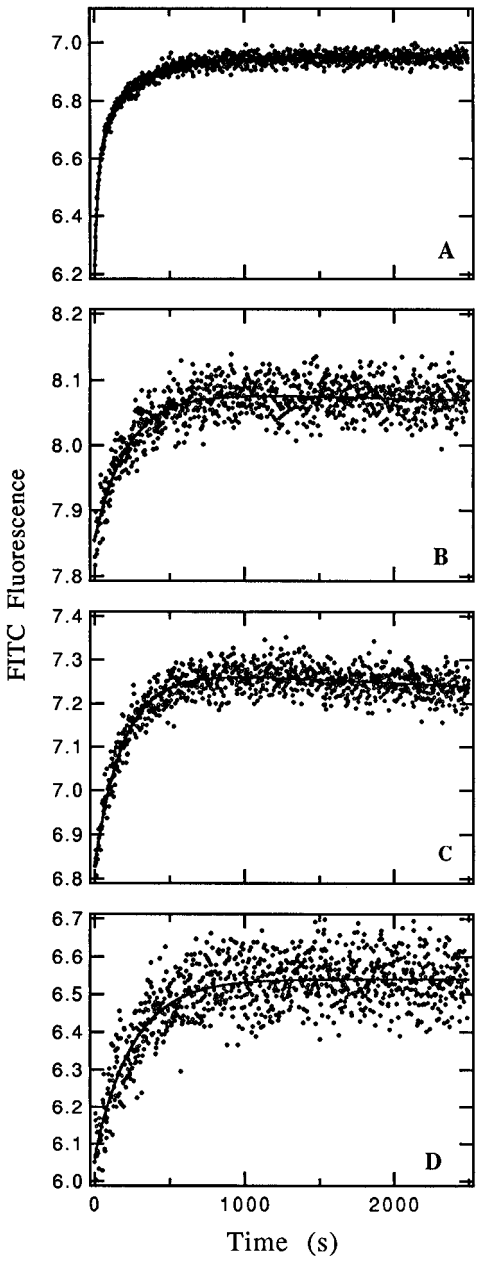

FIGURE 3: $(DCT)_2$-cys dissociation from FITC-anti-DNP IgE, $F(ab')_2$ fragments, and Fab′ fragments as monitored by fluorescence recovery. The FITC-IgE (or fragment) sample was pre-incubated with $(DCT)_2$-cys until fluorescence quenching due to binding was essentially complete. At $t = 0$, excess DCT was added to induce $(DCT)_2$-cys dissociation. Equations 6 and 9 were used to obtain theoretical fits (solid lines) of the data points. (A) FITC-IgE (16 nM; 32 nM in binding sites) pre-incubated with stoichiometric amounts of $(DCT)_2$-cys (15 nM; 30 nM in DNP groups) before addition of excess DCT (9 μM). The fit with eq 6 yields best values: $k_{-1} = (4.0 \pm 0.1) \times 10^{-3}$ s^{-1}; $4j_{-2} = (3.7 \pm 0.2) \times 10^{-2}$ s^{-1}; $A = 0.42$; $F_{max} = 6.95$; $F_{min} = 6.21$; $s = 0$. (B) FITC-Fab′ (32 nM) was incubated with stoichiometric amounts of $(DCT)_2$-cys (15 nM) before addition of large excess DCT (9 μM). The fit with eq 5 yields best values: $k_{-1} = (4.4 \pm 0.2) \times 10^{-3}$ s^{-1}; $F_{max} = 8.08$; $F_{min} = 7.86$; $s = -5.8 \times 10^{-6}$ s^{-1}. (C) Low concentration of FITC-IgE (1 nM) pre-incubated with high concentration of $(DCT)_2$-cys (100 nM) before addition of large excess of DCT (14 μM). The fit with eq 5 yields best values: $k_{-1} = (5.1 \pm 0.2) \times 10^{-3}$ s^{-1}; $F_{max} = 7.28$; $F_{min} = 6.83$; $s = -1.6 \times 10^{-5}$ s^{-1}. (D) FITC-$F(ab')_2$ (15 nM) pre-incubated with stoichiometric amounts of $(DCT)_2$-cys (15 nM) before addition of DCT (9 μM). The fit with eq 5 yields best values: $k_{-1} = (3.9 \pm 0.1) \times 10^{-3}$ s^{-1}; $F_{max} = 6.54$; $F_{min} = 6.07$; $s = 0$. The more noisy data for samples in B−D compared to the IgE sample in A are primarily due to lower stoichiometry of FITC labeling for the Fab fragments (B) and $F(ab')_2$ fragments (D) or lower IgE concentration (C).

Table 1: Rate Constants Determined for Single-Exponential Dissociation of $(DCT)_2$-cys from Anti-DNP IgE and Its $F(ab')_2$ and Fab′ Fragments[a]

anti-DNP	[anti-DNP] (nM)[b]	[$(DCT)_2$-cys] (nM)[b]	$k_{-1} = k_{-2}$ (10^{-3} s^{-1})[c]
Fab′	5	3.9	3.5 ± 0.2
Fab′	5	3.6	4.7 ± 0.2
Fab′	5	3.6	4.5 ± 0.1
Fab′	5	3.6	3.9 ± 0.1
Fab′	5	26	4.4 ± 0.2
Fab′	16	15	4.3 ± 0.3
Fab′	16	16	3.1 ± 0.1
Fab′	17	17	5.2 ± 0.2
Fab′	32	30	4.4 ± 0.2
IgE	2	200	5.7 ± 0.3
IgE	2	200	5.1 ± 0.2
IgE	4	400	5.0 ± 0.2
$F(ab')_2$	9	9	4.9 ± 0.1
$F(ab')_2$	30	29	3.9 ± 0.1
$F(ab')_2$	30	29	4.0 ± 0.1

[a] Anti-DNP IgE derivatives were pre-equilibrated with $(DCT)_2$-cys in indicated amounts before addition of excess DCT (9−14 μM) to drive $(DCT)_2$-cys dissociation. Each line represents a single independent experiment. [b] Concentrations are given in terms of sites: ligand binding sites on the IgE derivatives or DNP groups on the $(DCT)_2$-cys. [c] Dissociation rate constant determined from best fits of data with eq 5. Estimates of the standard deviation of the parameters for individual experiments were obtained with the bootstrap method described by Efron and Tishirani (1986) and 100 simulations of the data. The arithmetic average values (with standard deviations from this average) are for Fab′, $k_{-1} = k_{-2} = (4.2 \pm 0.7) \times 10^{-3}$ s^{-1}; for $F(ab')_2$, $k_{-1} = k_{-2} = (4.3 \pm 0.6) \times 10^{-3}$ s^{-1}; for IgE, $k_{-1} = (5.3 \pm 0.4) \times 10^{-3}$ s^{-1}.

single kinetic coefficient obtained for Fab′ is similar to the lower value observed with intact IgE. The experiment shown was carried out under conditions for maximal cross-linking (eq 2) such that at least 17% of the Fab′ are estimated to be cross-linked (see Appendix); these cross-linked sites make up at least 30% of all sites that were bound when dissociation was initiated at $t = 0$. Thus it appears that both the breaking of the cross-link and the dissociation of the monovalently bound ligand occur with the same reverse rate constants, i.e., $k_{-1} = k_{-2}$ (Figure 2A). As summarized in Table 1, a similar single-exponential dissociation process was observed at several concentrations of Fab′ and $(DCT)_2$-cys. The average value for the dissociation rate constant derived from these experiments is $k_{-1} = k_{-2} = (4.2 \pm 0.6) \times 10^{-3}$ s^{-1}.

We directly tested whether two kinetic coefficients, if present, could be detected for the range of cross-linked Fab′ sites initially present in the experiments of Table 1 by simulating data over the range of these initial conditions with eq 5 and adding random noise at levels typically encountered in our experiments. The kinetic coefficients used to generate the data were 3×10^{-2} s^{-1} and 3×10^{-3} s^{-1}, values similar to those determined for IgE. The simulated data containing noise were then fit with either a single (eq 6) or a double (eq 5) exponential function. In every case the single-exponential fit was readily rejected (systematic errors at short times), and the two set kinetic coefficients were recovered from the two-exponential fit which had a substantially reduced sum of squares (data not shown). These simulations further support the validity of the single exponential fits we determined for $(DCT)_2$-cys dissociation from Fab′ (Table 1).

The information provided by the Fab′ experiments allows definitive assignment of the two kinetic coefficients observed in the experiments with intact IgE described above. Thus for IgE and $(DCT)_2$-cys, $k_{-1} = k_{-2} = (4.4 \pm 0.3) \times 10^{-3}$ s^{-1} and $4j_{-2} = (4.7 \pm 0.7) \times 10^{-2}$ s^{-1}.

To evaluate k_{-1} directly for intact IgE we monitored dissociation of $(DCT)_2$-cys from FITC-IgE, when the $(DCT)_2$-cys is in excess by 100-fold (Figure 3C). Under these conditions, essentially all of the $(DCT)_2$-cys are expected to be monovalently bound to the FITC-IgE (Posner et al., 1995). Consistent with this expectation, the data are well-fitted by the single-exponential expression of eq 6. Furthermore, the kinetic coefficient that fits the data corresponds to the lower value obtained when FITC-IgE and $(DCT)_2$-cys are combined in stoichiometric amounts and is similar to the value obtained for $(DCT)_2$-cys and Fab′ fragments. Table 1 includes data from three experiments with intact IgE and excess $(DCT)_2$-cys. The average value for the dissociation rate constant from these experiments is $k_{-1} = (5.3 \pm 0.4) \times 10^{-3}$ s^{-1}.

The foregoing results indicate that IgE cross-linked with $(DCT)_2$-cys exhibits two kinetic coefficients (Figure 3A) because cyclization can occur with this bivalent species (Figure 2). Therefore, we were initially surprised to observe that for samples containing stoichiometric amounts of $(DCT)_2$-cys and bivalent $F(ab')_2$ fragments, the dissociation of $(DCT)_2$-cys is well-fitted by a single-exponential process similar to that observed with monovalent Fab′ fragments (Figure 3D). Similar results from three different experiments are included in Table 1, yielding an average value of (4.3 ± 0.6) × 10^{-3} s^{-1} for the kinetic coefficient.

One possible explanation for this result is that cyclic dimers do not form with $(DCT)_2$-cys and $F(ab')_2$ such that the dissociation is described simply by $k_{-1} = k_{-2}$. An alternative explanation is that cyclic dimers do form with both bivalent species but that the IgE−Fc segments increase the dissociation rate of cyclic dimers formed with this IgE $((DCT)_2\text{-cys}-\text{intact IgE})_2$ compared to cyclic dimers with its $F(ab')_2$ fragment $((DCT)_2\text{-cys}-F(ab')_2)_2$. This latter explanation would correspond to $k_{-1} = k_{-2} < j_{-2}$ for IgE (eq 6), whereas $k_{-1} = k_{-2} = j_{-2}$ for $F(ab')_2$ (eq 9).

Gel Filtration of FITC-IgE and FITC-IgE F(ab′)$_2$ Bound to (DCT)$_2$-cys. If cyclic dimers form readily with the $F(ab')_2$ fragments, then we would expect these to be highly stable, as was determined for $(DCT)_2$-cys and intact IgE bound to FcεRI on cells (Posner et al., 1995). We evaluated this possibility for soluble IgE and its $F(ab')_2$ fragments by gel filtration chromatography which separates molecules with different molecular sizes (as represented by their apparent Stokes radii). For these purposes FITC-IgE or $F(ab')_2$ fragments were pre-incubated (or not) with stoichiometric amounts of $(DCT)_2$-cys, at relatively high concentrations to maximize the amount of binding and cross-linking.

As seen in Figure 4A (trace a) FITC-IgE alone shows a single peak at a retention time of 30 min. This peak appears as expected for monomeric IgE of molecular mass ∼180 kDa on the basis of the gel filtration standards. When FITC-IgE is pre-incubated with $(DCT)_2$-cys, a second peak appears at a retention time of 26 min (Figure 4A, trace b), which is consistent with dimeric IgE of molecular mass 360 kDa. No significant peaks corresponding to larger molecular masses are detected. As seen in Figure 4B (trace a), FITC-$F(ab')_2$ fragments alone show a single peak at a retention time of 31 min as expected for a monomeric $F(ab')_2$ of molecular mass 120 kDa. When FITC-$F(ab')_2$ is pre-incubated with $(DCT)_2$-cys, a second peak appears at a retention time of 28 min which is consistent with a dimeric $F(ab')_2$ of molecular

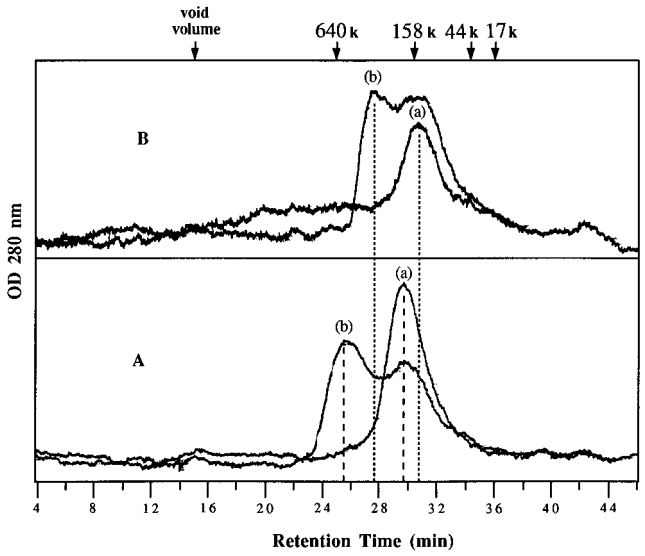

FIGURE 4: Superose 6 gel filtration chromatography of (A) FITC-IgE and (B) FITC-F(ab′)$_2$ without (a traces) or with (b traces) pre-incubation with a stoichiometric amount of (DCT)$_2$-cys for 30 min at room temperature. Samples were analyzed under identical conditions as described in Materials and Methods. The retention times for molecular mass standards are indicated on the upper *x*-axis. The *y*-axes have different scales for A and B.

mass 240 kDa (Figure 4B, trace b). For both IgE and F(ab′)$_2$, somewhat more than half of the protein is eluted at the dimer size after the incubation with equimolar (DCT)$_2$-cys and after gel filtration which will separate any ligand dissociated during the ~30 min chromatography process. These results support previous observations that double-bonded, cyclic dimers are highly stable for IgE combined with (DCT)$_2$-cys in solution (Posner et al., 1991), and they also show that F(ab′)$_2$ forms highly stable cyclic dimers with (DCT)$_2$-cys. As discussed further below, we expect these double-bonded complexes to outlast any linear aggregates connected by single bonds which would dissociate during the time period of the chromatographic separation.

DISCUSSION

The symmetric bivalent ligand (DCT)$_2$-cys has been valuable for relating the binding properties of IgE to its structural and functional properties. Our previous studies showed that (DCT)$_2$-cys forms stable cyclic dimers with IgE bound to FcϵRI on the RBL cell surface (Erickson et al., 1991; Posner et al., 1995) and quite likely with IgE in solution (Posner et al., 1991). These results are consistent with studies by Schweitzer-Stenner and colleagues (1987, 1992a,b) who also found that different small DNP bivalent ligands and anti-DNP IgE mAb aggregate predominantly into cyclic dimers in solution. Studies with mouse IgG subclasses specific for 1,5-dansyl haptens also showed efficient formation of cyclic complexes between these IgG antibodies and symmetrical bivalent haptens (Phillips et al., 1990). The more restricted segmental flexibility of IgE antibodies (Oi et al., 1984; Holowka et al., 1990) suggests that the formation of cyclic complexes may require a longer bivalent ligand to overcome steric limitations that are more significant for the IgE class. Cyclic dimers with (DCT)$_2$-cys and IgE on RBL cells appear to be incapable of triggering Ca^{2+} mobilization or degranulation even when they are cross-linked into higher aggregate states, whereas linear aggregates formed at high concentrations of this ligand are functional (Posner et al., 1995). Structural limitations of the aggregated cyclic dimers may explain this functional ineffectiveness.

Dissociation of (DCT)$_2$-cys from IgE in solution was shown previously to occur with a faster [$(4.8 \pm 3.2) \times 10^{-2}$ s^{-1}] and a slower [$(5.6 \pm 1.9) \times 10^{-3}$ s^{-1}] kinetic coefficient (Posner et al., 1991),[3] and these values are similar to those obtained for IgE bound to FcϵRI on RBL cells (Erickson et al., 1991). As we postulated previously, these results could be explained by the formation of highly stable cyclic dimers. The monovalent analogue, DCT, dissociates from IgE with a single rate constant, $k_{-1} = 2.6 \pm 0.1 \times 10^{-2}$ s^{-1} (Goldstein et al., 1989), and this was consistent with the faster kinetic coefficient observed with (DCT)$_2$-cys corresponding to the dissociation of the monovalently bound bivalent ligand (Posner et al., 1991). The present study examined this dissociation process directly for IgE in solution by comparing the dissociation of (DCT)$_2$-cys from intact bivalent IgE, monovalent Fab′ fragments, and bivalent F(ab′)$_2$ fragments. We confirmed two kinetic coefficients for IgE and (DCT)$_2$-cys with average values of $(4.7 \pm 0.7) \times 10^{-2}$ s^{-1} and $(4.4 \pm 0.3) \times 10^{-3}$ s^{-1} that are the same as those observed previously, as expected. Furthermore, we showed that these values are independent of enhanced quenching that appears to occur with bound sites in cyclic dimers compared to other types of bound sites (Appendix). Finally, we could identify definitively the dissociation steps corresponding to these two kinetic coefficients.

Previous binding data together with those presented here (Figure 3; Table 1) are self-consistent with the following description. The Fab′ fragments can bind (DCT)$_2$-cys monovalently or be cross-linked by (DCT)$_2$-cys into linear dimers (Figure 2A). The rate constant for breaking of the cross-link is the same as dissociation of the monovalently bound bivalent ligand, i.e., $k_{-2} = k_{-1} = (4.2 \pm 0.6) \times 10^{-3}$ s^{-1} and different from the rate constant observed for the dissociation of DCT. This corrected assignment for $k_{-2} = k_{-1}$ is consistent with that suggested by Schweitzer-Stenner and colleagues (1992b). IgE can bind (DCT)$_2$-cys monovalently and also form linear dimers similarly to the Fab′ fragments; IgE has the same values as Fab′ for $k_{-2} = k_{-1} = (4.4 \pm 0.3) \times 10^{-3}$ s^{-1}. IgE can additionally form cyclic dimers (Figure 2B), and the rate constant for the breaking of this ring is $4j_{-2} = (4.7 \pm 0.7) \times 10^{-2}$ s^{-1} or $j_{-2} = (1.2 \pm 0.2) \times 10^{-2}$ s^{-1}. Thus breaking a (DCT)$_2$-cys bond to convert a cyclic dimer of IgE to a linear dimer (corresponding to j_{-2}) is about three times faster than breaking a cross-link in a linear chain (k_{-2}) or dissociation of the monovalently bound bivalent ligand (k_{-1}).

Bivalent F(ab′)$_2$ combined with (DCT)$_2$-cys in stoichiometric amounts would be expected to form both linear chains and cyclic dimers similarly to IgE. The observation that (DCT)$_2$-cys dissociation from F(ab′)$_2$ occurs as a single-exponential process, similar to that for Fab′ and different from that for IgE, indicates that the Fc segments affect the dissociation rate of the cyclic dimer state. Strong evidence that F(ab′)$_2$ forms cyclic dimers with high stability, similar to those formed by IgE, is provided by gel filtration chromatography, which shows similar amounts of monomeric and dimeric species after pre-incubation with (DCT)$_2$-cys (Figure 4). The dimer peaks comprise primarily cyclic dimers because singly bonded linear chains would break up during the time of chromatographic separation as predicted by the observed dissociation rate constant $k_{-2} = 4 \times 10^{-3}$ s^{-1} which corresponds to a half-life ($t_{1/2}$) of ~200 s ($t_{1/2} =$

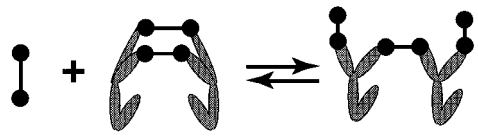

FIGURE 5: Reversible reaction between cyclic dimers and linear dimers. When the free bivalent ligand concentration is large, the addition of more ligand leads to a reduction in the concentration of cyclic dimers.

$0.69/k_{-2}$). The dimer peak is observed after 26 min or $8t_{1/2}$ for IgE and after 31 min or $9t_{1/2}$ for F(ab′)$_2$, such that nearly complete dissociation linear chains and separation of monomeric units would be expected. The cyclic dimers are substantially more stable species because of their double-bond attachment and enhanced possibility for rebinding. Separation of the two IgE or F(ab′)$_2$ in this case would require that, after the first bond breaks, the second bond must also break before the first bond reforms. The fact that we observe a dimer peak that is similar in magnitude to the monomer peak indicates that the rate constant for ring formation (j_{+2}; see Figure 2B) is large compared to j_{-2} and k_{-2}. This is consistent with a large value for the equilibrium constant for cyclic dimer formation ($J_2 = j_{+2}/j_{-2}$) that was observed for (DCT)$_2$-cys and IgE−FcϵRI on cells (Posner et al., 1995).

We previously showed by resonance energy transfer that rodent IgE has a bent conformation both in solution and when bound to FcϵRI on the RBL cell membrane surface (Zheng et al., 1992), and this bent structure has recently been confirmed with hydrodynamic methods for human IgE in solution (Beavil et al., 1995). Two such bent IgE that are dimerized into a ring by a pair of bivalent ligands could place the Fc regions close together (Figure 5). This structural arrangement is consistent with the inter-IgE energy transfer observed for anti-dansyl IgE bound to FcϵRI on RBL cell membranes and a short dansyl bivalent ligand when the donor and acceptor probes were placed at the hinge and C-terminus of IgE (Zheng, 1992; Baird et al., 1993). Such proximity could result in Fc−Fc interactions that have stabilizing or destabilizing influence on the ring structure. Our binding studies on the soluble proteins indicate $k_{-1} = k_{-2} = j_{-2}$ for F(ab′)$_2$ but $k_{-1} = k_{-2} < j_{-2}$ for IgE when cyclic dimers are present. This difference between F(ab′)$_2$ and IgE indicates that Fc segments that can be apposed in cyclic dimers of IgE interact unfavorably, probably because of steric hindrance. IgE in solution are not subject to the same orientational constraints that are placed on IgE bound to FcϵRI on cell surfaces. Thus it is likely that the bent IgE in solution form cyclic dimers of both types with Fc segments facing each other, resembling an O shape, and Fc facing in opposite directions, resembling an S shape in sideways profiles. Only those with the apposed Fc (O shape) would be expected to show the faster dissociation rate, such that $k_{-1} = k_{-2} < j_{-2}$. For the other type of cyclic dimers (S shape) we would expect $k_{-1} = k_{-2} = j_{-2}$. In other words, the faster dissociation rate that is clearly observed for IgE probably represents only a portion of the cyclic dimers present. For the F(ab′)$_2$ the two types of cyclic dimers are invisible without the Fc being present to cause possible interference and thus a faster dissociation rate.

Evidence for noncovalent Fc−Fc interactions was obtained previously in the case of mouse IgG subclass 3 when it was observed that IgG3 mAb associate more tightly to antigens displayed on a surface when compared to other IgG subclasses with the same specificity (Greenspan et al., 1992; Cooper et al., 1994). For the IgG3 subclass this Fc−Fc interaction appears to have a stabilizing effect on immune complex formation, whereas the Fc−Fc interaction we detect for cyclic dimers of IgE appears to cause some steric strain.

In summary, our comparison of (DCT)$_2$-cys binding to Fab′ and F(ab′)$_2$ supports previous results indicating that IgE in solution is cross-linked by (DCT)$_2$-cys into aggregates that are dominated by stable cyclic dimers. In the present experiments, we find that breaking a ring-forming cross-link occurs with a dissociation constant $j_{-2} \simeq 1 \times 10^{-2}$ s^{-1}, whereas breaking a linear cross-link or dissociating the monovalently-bound bivalent ligand occurs with somewhat lower, indistinguishable rate constants, $k_{-1} = k_{-2} \simeq 4 \times 10^{-3}$ s^{-1}. Our results indicate that the Fc segments of IgE can be apposed in the cyclic dimers and cause steric strain that apparently does not preclude the formation of this stable complex but increases the dissociation rate by a factor of 2−3.

Our previous finding that (DCT)$_2$-cys dissociates from IgE in solution and IgE bound to FcϵRI on RBL cells with very similar kinetic coefficients suggests that the identification of binding processes we have made here for soluble IgE can be generalized correspondingly to the cell surface. Ligand-mediated cross-linking of IgE−FcϵRI leading to apposition and physical interference of IgE−Fc segments could limit critical interactions between these cross-linked FcϵRI. For example, we found that the very stable cyclic dimers of IgE−FcϵRI formed by (DCT)$_2$-cys are functionally ineffective (Posner et al., 1995), and this could be due, for example, to the inability of such complexes to undergo transphosphorylation that occurs efficiently with other multivalent ligands (Pribluda et al., 1994). This suggests that the bent conformation of IgE plays a more general role in influencing the formation of effective aggregates with physiological antigens: the functionally effective aggregates may comprise IgE−FcϵRI that are cross-linked into complexes such that the IgE−Fc can assume positions that are not rigidly apposed. The present results suggest new ways to assess the structural basis for effective signaling by cross-linked IgE−FcϵRI complexes.

APPENDIX

Equilibrium Binding of Fab′ Fragments to Bivalent Ligands. We estimate the equilibrium concentration of Fab′ fragments that are cross-linked by symmetric bivalent ligands in the following way. We call the concentrations of free and total (DCT)$_2$-cys, C and C_T, respectively, and the concentrations of free and total Fab′ as R and R_T, respectively. Note that in eq 2 $R_T = [\text{Fab}']_{\text{Total}}$. The concentration of singly bound ligand−Fab′ complexes is then $2K_1CR$, and the concentration of aggregates (two Fab′ cross-linked by one (DCT)$_2$-cys) is $K_1CK_2R^2$. Therefore,

$$R_T = R + 2K_1CR + 2K_1CK_2R^2 \qquad \text{(A1)}$$

$$C_T = C + 2K_1CR + K_1CK_2R^2 \qquad \text{(A2)}$$

where the single-site equilibrium constants for binding and cross-linking are, respectively, $K_1 = k_{+1}/k_{-1}$ and $K_2 = k_{+2}/k_{-2}$ (see Figure 2A). Solving eq A2 for C and substituting into eq A1 we obtain

$$R_T = R + C_T(2K_1R + 2K_1K_2R^2)/(1 + 2K_1R + K_1K_2R^2) \quad (A3)$$

To calculate the concentrations of Fab′ that are singly bound and cross-linked we numerically solve eq A3 for R. We then substitute this value of R into eq A2 to obtain C. For $(DCT)_2$-cys in solution we take $K_1 = 2 \times 10^9$ M^{-1} and $K_2 = 3 \times 10^7$ M^{-1} (Erickson et al., 1986; see footnote 4). When $C_T = 15$ nM (a DNP concentration of 30 nM) and $R_T = 32$ nM, numerically solving eq A3 gives $R = 14.6$ nM and substituting into eq A2 gives $C = 0.21$ nM. With these values we find that at equilibrium 54.5% of the Fab′ sites are bound, 37.9% are singly bound, and 16.6% are in cross-links. Thus, 30.4% of all bound sites are in cross-links.[4]

For the special case when cross-linking is maximum, analytic solutions for eqs A1 and A2 can be obtained. We summarize here the results for Fab′ without proof; the proof is similar to that for IgE published previously (Dembo & Goldstein, 1978). When cross-linking is maximum, the free bivalent ligand concentration is given by $C = 1/(2K_1)$ and the total bivalent ligand concentration, C_T, is given by eq 2. When cross-linking is maximum, the concentration of Fab′ not cross-linked (either free or singly bound), W, is

$$W = 2(-1 + \sqrt{1 + K_2R_T})/K_2 \quad (A4)$$

The concentration of bound sites on singly bound ligands is $W/2$, and the concentration of bound sites on doubly bound ligands is $K_2W^2/2$. For example, if as before $R_T = 32$ nM, $K_1 = 2 \times 10^9$ M^{-1}, and $K_2 = 3 \times 10^7$ M^{-1}, then from eq 2 the total ligand concentration at which cross-linking is maximum equals 16.25 nM. From eq A4 $W = 26.7$ nM, so the fraction of Fab′ sites not cross-linked, $W/R_T = 0.833$, and the fraction cross-linked, $1 - W/R_T = 0.167$. The fraction of Fab′ sites singly bound, $W/(2R_T) = 0.417$ so that of all bound sites, 28.6% are cross-linked.[4]

A Bound Site in a Cyclic Complex Quenches More Strongly than Other Bound Sites. If all bound sites quench the same, then the fluorescence should be a monotonically decreasing function of the bivalent ligand concentration because increasing this concentration always causes more sites to be bound until saturation. Thus, in a series of additions of bivalent ligand, such as in Figure 6A, after each addition the fluorescence should monotonically decrease. However, if a bound site in a cyclic complex quenches more strongly than other bound sites, the possibility arises that at a high bivalent ligand concentration, adding additional ligand might cause an increase in fluorescence. This would occur if (1) the addition favors the right side of the reaction shown in Figure 5, causing a decrease in the concentration of sites bound in cyclic complexes and an increase in other bound states, and (2) the gain in fluorescence due to this conversion from bound sites in cyclic complexes to other types of bound sites is sufficient to offset the decrease in fluorescence caused by an increase in the total number of bound sites.

In the experiment shown in Figure 6A, $(DCT)_2$-cys was added sequentially, first 200 nM, then 550 nM, and finally 880 nM. After the final addition we observed a decrease

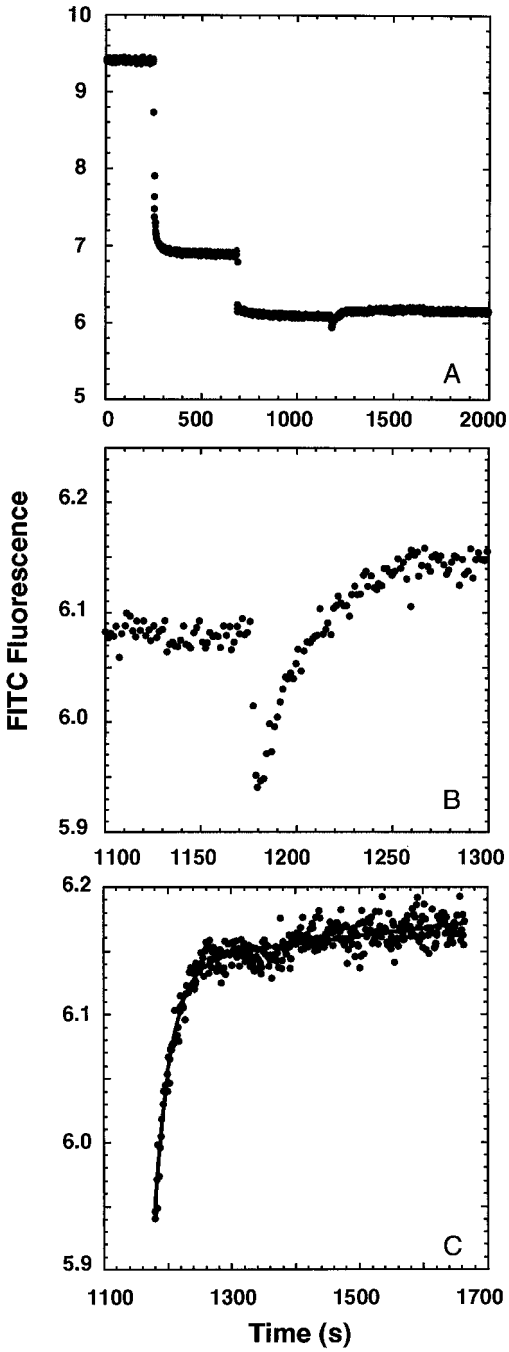

FIGURE 6: $(DCT)_2$-cys binding to 200 nM FITC-anti-DNP IgE in solution as monitored by fluorescence quenching. (A) At $t = 249$, 686, and 1176 s $(DCT)_2$-cys was added to yield total concentrations of 200, 550, and 880 nM, respectively. (B) Enlargement of the fluorescence recovery observed after the final addition of $(DCT)_2$-cys at $t = 1176$ s. (C) Single-exponential fit (similar to eq 6) of the fluorescence recovery curve occurring after the final $(DCT)_2$-cys addition. Best fit values of the parameters are as follows: kinetic coefficient $= 3.9 \times 10^{-2}$ s^{-1}; $s = 6.1 \times 10^{-5}$ s^{-1}; starting fluorescence = 5.93; final fluorescence = 6.13.

followed by a recovery of fluorescence (Figure 6A; enlarged in Figure 6B). The initial, rapid decrease was due to the immediate filling of a small number of remaining Fab′ sites as well as dilution caused by the small increase in volume of the sample. (When buffer alone was added after the last addition of DCT a small decrease with no recovery was observed; data not shown). The slower recovery phase we attribute to the breaking of bounds in cyclic complexes (as depicted in Figure 5). When the recovery portion of the curve is fitted with a single-exponential function (similar to

[4] Our recent and more extensive investigation of K_2 for Fab′ and $(DCT)_2$-cys in solution shows the value for this parameter to be significantly higher than 3×10^7 M^{-1}. Calculations based on this lower value yield lower limits for the fraction of total Fab′ in cross-linked aggregates.

eq 6; Figure 6C) the value obtained for the kinetic coefficient is approximately equal to that of the faster kinetic coefficient ($4j_{-2}$). For the recovery curve in Figure 6C plus five additional recovery curves observed in similar experiments (data not shown) we found the kinetic coefficient to be (3.5 ± 0.6) $\times 10^{-2}$ s^{-1}, which is in agreement with the kinetic coefficient $4j_{-2} = (4.7 \pm 0.7) \times 10^{-2}$ s^{-1}, we obtained for the breaking of bonds in IgE−$(DCT)_2$-cys cyclic complexes (see Results Section).

Independence of Kinetic Coefficients on Differential Quenching. It is important to note, as we did in the Materials and Methods section, that eq 9 is correct whether or not all bound sites of the bivalent ligand quench equally. This can be demonstrated as follows. The fraction of sites bound is a sum of three terms.

$$f_b = y_1 + 2y_2 + 2y_3 \tag{A5}$$

where y_1, y_2, and y_3 are, respectively, the fraction of bivalent ligands singly bound, doubly bound in chains, and doubly bound in cyclic complexes. If a is the fraction of bound sites in cyclic dimers when DCT is added, then

$$y_3 = a \exp(-4j_{-2}t) \tag{A6}$$

$$y_1 + 2y_2 = (1 - \alpha a)\exp(-k_{-1}t) + \alpha(1 - \alpha)\exp(-4j_{-2}t) \tag{A7}$$

$$\alpha = (k_{-1} - 3j_{-2})(k_{-1} - j_{-2})/[(k_{-1} - 2j_{-2})(k_{-1} - 4j_{-2})] \tag{A8}$$

Note that if we sum eqs A6 and A7 we recover eqs 7 and 8.

We define ΔF_1, ΔF_2, and ΔF_3 as the difference in fluorescence between a bond formed by a monovalent ligand (DCT) and either a bond formed by a singly bound bivalent ligand (ΔF_1), a doubly bound bivalent ligand in a chain (ΔF_2), or a doubly bound bivalent ligand in a cyclic complex (ΔF_3). We assume that $\Delta F_1 = \Delta F_2$, i.e., all bound sites not in cyclic complexes quench the same. Then

$$F = F_{max} - \Delta F_1[(y_1 + 2y_2) + r(y_3)] \tag{A9}$$

where

$$r = \Delta F_3/\Delta F_1 = (F_{max} - F_r)/(F_{max} - F_s) \tag{A10}$$

F_{max} is, as defined previously for eq 5, the fluorescence when all IgE sites are bound with DCT; F_s is the fluorescence when all sites are filled by singly bound bivalent ligands; F_r is the fluorescence when all sites are bound in cyclic complexes. If a bound site in a cyclic complex quenches more strongly than a bound site not in a cyclic complex, $r > 1$; if it quenches the same, $r = 1$; and if it quenches less, $r < 1$.

If one sets $t = 0$ in eq A9 (when $F = F_{min}$ as defined previously for eq 5), solves for ΔF_1, and then substitutes this expression back into eq A9, one can show that

$$F = F_{max} - (F_{max} - F_{min})(A \exp(-k_{-1}t) + (1 - A)\exp(-4j_{-2}t)) \tag{A11}$$

where

$$A = (1 - \alpha a)/(1 - a + ar) \tag{A12}$$

Table 2: Effect on the Interpretation of Amplitude A When Bound Sites in Cyclic Complexes Quench More Strongly Than Bound Sites in Open Configurations[a]

r	a_1	a_2	a_3	a_4
1.00	1.03	1.49	2.14	2.75
2.00	0.22	0.35	0.60	0.94
3.00	0.12	0.20	0.35	0.56
4.00	0.09	0.14	0.25	0.40
5.00	0.07	0.11	0.19	0.34
6.00	0.05	0.09	0.15	0.26

[a] Four experiments were fitted simultaneously with eq 9: (1) [IgE] = 2 nM, [$(DCT)_2$-cys] = 200 nM; (2) [IgE] = 4 nM, [$(DCT)_2$-cys] = 400 nM; (3) [IgE] = 40 nM, [$(DCT)_2$-cys] = 39 nM; (4) [IgE] = 32 nM, [$(DCT)_2$-cys] = 30 nM. The best fit values obtained for the kinetic coefficients were $k_{-1} = 4.2 \times 10^{-3}$ s^{-1} and $4j_{-2} = 2.9 \times 10^{-2}$ s^{-1}. The respective best fit values for the amplitudes were $A_1 = 0.78$, $A_2 = 0.68$, $A_3 = 0.55$, $A_4 = 0.41$, where A_i is the value of A for the ith experiment. Listed for these values of A_i are the values of a_i, the fraction of bound sites in cyclic complexes at the start of the experiment, for different fixed values of r (see eqs A10 and A12). To account for instrumental drift s was also allowed to vary in eq 9. For the four separate experiments $s_1 = -1.6 \times 10^{-5}$ s^{-1}, $s_2 = 6.0 \times 10^{-6}$ s^{-1}, $s_3 = 2.1 \times 10^{-5}$ s^{-1}, and $s_4 = 3.4 \times 10^{-6}$ s^{-1}.

Equation A11 accounts for possible differential quenching and has the same form, including the same kinetic coefficients, as eq 9. The difference between eq 9 and eq A11 resides in the definition of A. Note that when $r = 1$ eq A12 reduces to eq 8.

Interrelationship between a and r. Equation A12 shows that from dissociation experiments one cannot separately determine a and r but only the weighted sum A. To illustrate this point we fitted four IgE−$(DCT)_2$-cys dissociation experiments simultaneously with eq 9. For these experiments the best fit values of the kinetic coefficients are $k_{-1} = 4.2 \times 10^{-3}$ s^{-1} and $4j_{-2} = 2.9 \times 10^{-2}$ s^{-1}. For each experiment the best fit value of A was also determined from eq 9. In Table 2 we list the values of a that are obtained for different values of r. If there were no difference in quenching, $r = 1$, and from Table 2 we see that a is predicted to be greater than 1.0. This is a nonphysical result because a is the fraction of bound sites in cyclic complexes at the start of the experiment. However, if $r > 1$ we see that reasonable values for a less than 1.0 are obtained. This result plus the recovery curves of Figure 6 support the hypothesis that a bound site in a cyclic complex quenches more strongly than other types of bound sites.

One additional line of evidence for differential quenching comes from determining the following quantity:

$$q = (F_0 - F_{min})/(F_0 - F_{max}) \tag{A13}$$

where F_0 is the initial fluorescence before the addition of bivalent ligand when all sites are free, and F_{max} and F_{min} are as previously defined. For experiments 1 and 2 in Table 2, where bivalent ligand was in large excess, $q = 1.24$ and 1.26. For these experiments we expect essentially all sites to be bound by singly bound ligand before the addition of DCT. In experiments 3 and 4 the IgE concentrations were large and approximately equal to the bivalent ligand concentrations. These concentrations favor cyclic complex formation. When DCT was added there was a significant drop in fluorescence, indicating that some sites were free before the addition of DCT. Thus F_{min} for these experiments involves contributions from bivalent ligand bound in and out of cyclic complexes and sites bound by DCT. The q values obtained

were 1.45 and 1.33. For these q values to be larger than those in experiments 1 and 2 it is necessary that F_{min} be larger in experiments 1 and 2 than in experiments 3 and 4. This in turn implies that quenching by a bound site in a cyclic complex is greater (F_{min} lower) than that of other types of bound sites. Unfortunately, we cannot directly determine how much greater; because of equilibrium conditions at all concentrations of IgE and bivalent ligands it is not possible to set up an experiment where all sites are bound in cyclic complexes.

REFERENCES

Baird, B., Zheng, Y., & Holowka, D. (1993) *Acc. Chem. Res. 26*, 428−434.

Beavil, A. J., Young, R. J., Sutton, B. J., Perkins, S. J. (1995) *Biochemistry 34*, 14449.

Cooper, L. J. N., Robertson, D., Granzow, R., & Greenspan, N. S. (1994) *Mol. Immunol. 8*, 577−84.

Dembo, M., & Goldstein, B. (1978) *J. Immunol.* 121, 345−53.

Efron, B., & Tibshirani, R. (1986) *Stat. Sci. 1*, 54−77.

Erickson, J., Kane, P., Goldstein, B., Holowka, D., & Baird, B. (1986) *Mol. Immunol. 23*, 769−782.

Erickson, J. W., Posner, R. G., Goldstein, B., Holowka, D., & Baird, B. (1991) *Biochemistry 30*, 2357−2363.

Fewtrell, C., & Metzger, H. (1980) *J. Immunol. 125*, 701−710.

Goldstein, B. (1988) *Theoretical Immunology, Part One* (Perelson, A. S., Ed.) Addison Wesley, New York.

Goldstein, B., Posner, R., Torney, D., Erickson, J., Holowka, D., & Baird, B. (1989) *Biophys. J. 56*, 955−966.

Greenspan, N. S., Dacek, D. A., & Cooper, L. J. N. (1989) *FASEB 3*, 2203−2207.

Holowka, D., & Metzger, H. (1982) *Mol. Immunol. 19*, 219−227.

Holowka, D., & Baird, B. (1983) *Biochemistry 22*, 3466−3474.

Holowka, D., Wensel, T., & Baird, B. (1990) *Biochemistry 29*, 4607−12.

Kane, P., Erickson, J., Fewtrell, C., Baird, B., & Holowka, D. (1986) *Mol. Immunol. 23*, 783−790.

Liu, F., Bohn, J. W., Ferry, E. L., Yamamoto, H., Molinaro, C. A., Sherman, L. A., Klinman, N. R., & Katz, D. (1980) *J. Immunol. 124*, 2728−2736.

Myers, J. N., Holowka, D., & Baird, B. (1992) *Biochemistry 31*, 567−575.

Oi, V. T., Voung, T. M., Hardy, R., Reidler, J., Dangle, J., Herzenberg, L. A., & Stryer, L. (1984) *Nature 307*, 136−40.

Perelson, A., & DeLisi, C. (1980) *Math. Biosci. 48*, 71−110.

Perez-Montfort, R., & Metzger, H. (1982) *Mol. Immunol. 19*, 1113−1125.

Phillips, M. L., Oi, V. T., & Schumaker, V. N. (1990) *Mol. Immunol. 27*, 181−90.

Posner, R. G., Erickson, J. W., Holowka, D., Baird, B., & Goldstein, B. (1991) *Biochemistry 30*, 2348−2356.

Posner, R. G., Subramanian, K., Goldstein, B., Thomas, J., Feder, T., Holowka, D., & Baird, B. (1995) *J. Immunol. 155*, 3601−3609.

Pribluda, V. S., Pribluda, C., & Metzger, H. (1994) *Proc. Natl. Acad. Sci. U.S.A. 91*, 11246−50.

Schweitzer-Stenner, R., Luscher, I., & Pecht, I. (1987) *Biochemistry 26*, 3602−3612.

Schweitzer-Stenner, R., Licht, A., & Pecht, I. (1992a) *Biophys. J. 63*, 551−562.

Schweitzer-Stenner, R., Licht, A., & Pecht, I. (1992b) *Biophys. J. 63*, 563−568.

Zheng, Y. (1992) Ph.D. Thesis, Cornell University, Ithaca, NY.

Zheng, Y., Shopes, B., Holowka, D., & Baird, B. (1992) *Biochemistry 31*, 7446−7456.

BI9523522